# Synthesis, Characterization and Properties of High-Energy Compounds from Nitroisobutylglycerol

## Supporting information

**Sergey A. Rzhevskiy [1], Lidiya I. Minaeva [1], Maxim A. Topchiy [1], Igor N. Melnikov [2], Vitaly G. Kiselev [3], Alla N. Pivkina [2], Igor V. Fomenkov [4] and Andrey F. Asachenko [1,*]**

[1] A.V. Topchiev Institute of Petrochemical Synthesis, Russian Academy of Sciences, Leninsky Prospect 29, 119991, Moscow
[2] Semenov Federal Research Center for Chemical Physics RAS, 4 Kosygina Str., 119991 Moscow, Russia
[3] Institute of Chemical Kinetics and Combustion SB RAS, 3 Institutskaya Str., 630090 Novosibirsk, Russia
[4] Zelinsky Institute of Organic Chemistry RAS, 47 Leninsky Ave., 119991 Moscow, Russia
* Correspondence: aasachenko@ips.ac.ru.

## Table of content

Thermal behavior upon cooling for liquid samples .....S2

Thermochemical data.....S4

NMR spectra.....S5

**Thermal behavior upon cooling for liquid samples**

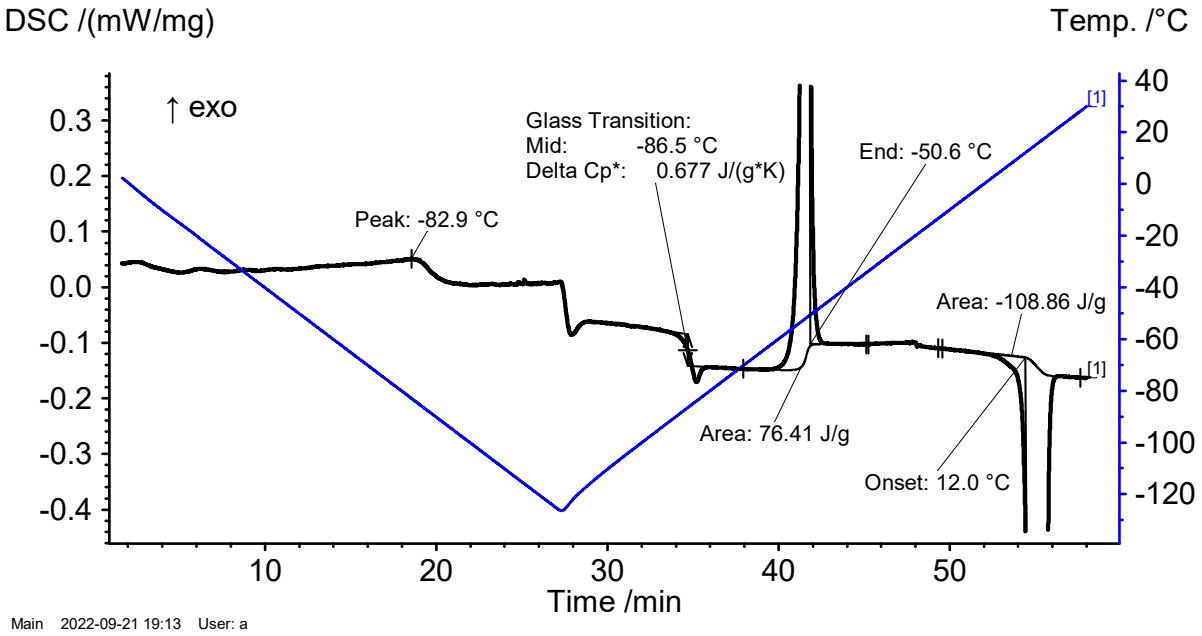


**Figure S1.** DSC (black curve) and a temperature time dependence (blue line) for the cooling-heating cycle of ANDP (7). The cooling and heating rates were 5 K $min^{-1}$. From left to the right: a vitrification effect, a DSC trace change due to a temperature program change (an experimental artefact), glass transition, cold crystallization, and melting (m.p. is 12°C).

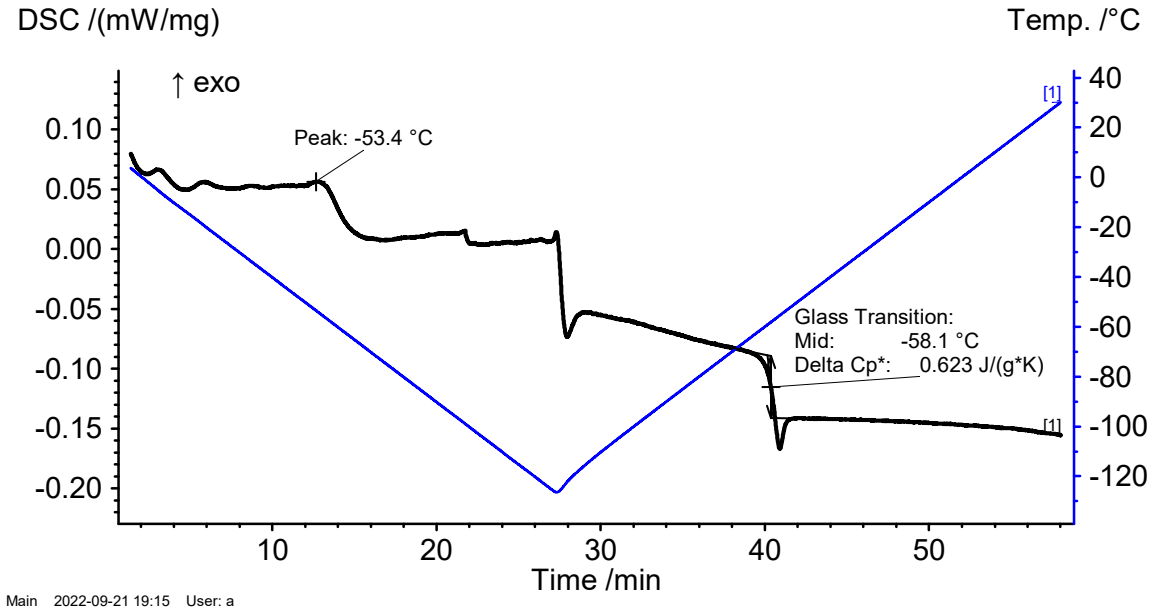


**Figure S2.** DSC (black curve) and a temperature time dependence (blue line) for the cooling-heating cycle of NIBTN (3). The cooling and heating rates were 5 K $min^{-1}$. From left to the right: a vitrification effect, DSC change due to a temperature program change (an experimental artefact), glass transition.

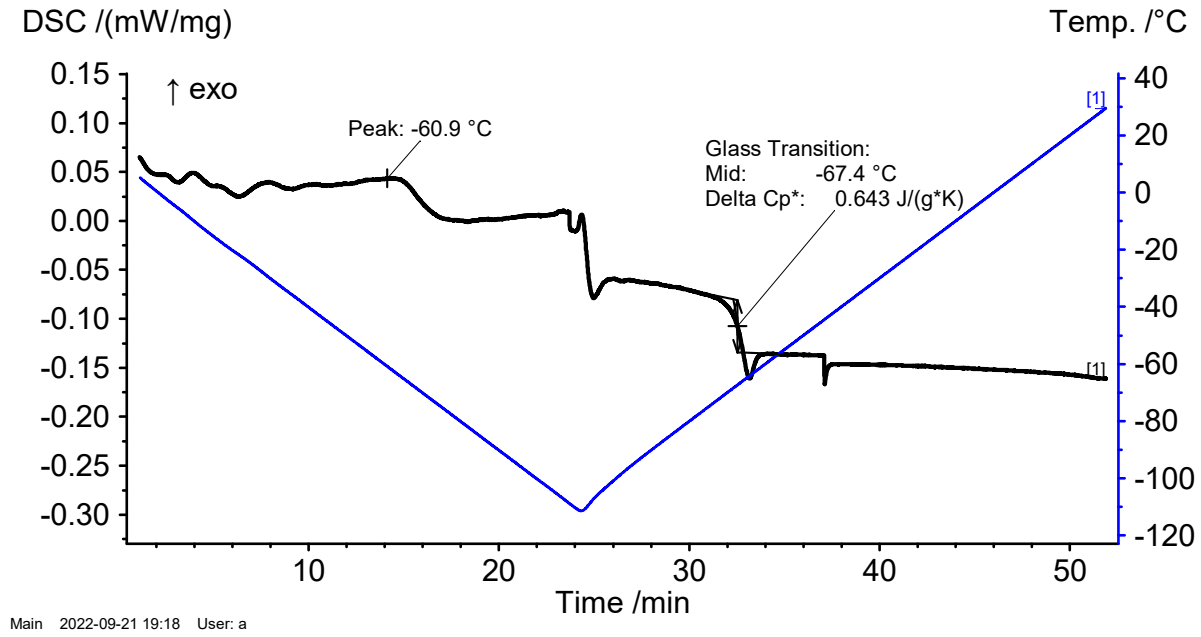


**Figure S3.** DSC (black curve) and a temperature time dependence (blue line) for the cooling-heating cycle of AMDNNM (6). The cooling and heating rates were 5 K $min^{-1}$. From left to the right: a vitrification effect, DSC change due to a temperature program change (an experimental artefact), glass transition.

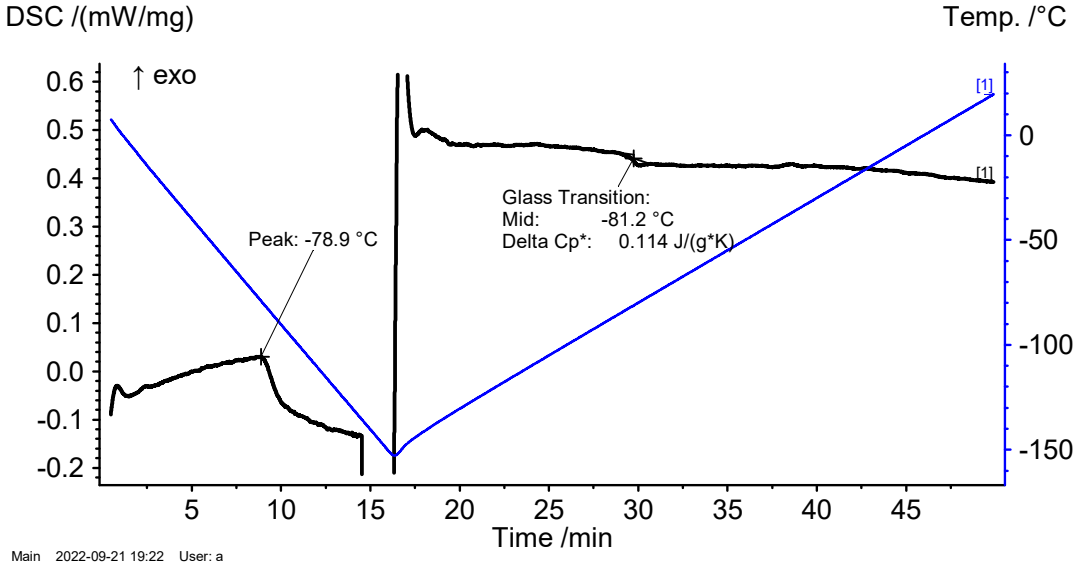


**Figure S4.** DSC (black curve) and a temperature time dependence (blue line) for the cooling-heating cycle of NPN (4). The cooling and heating rates were 5 K $min^{-1}$. From left to the right: vitrification effect, DSC change due to temperature program change (an experimental artefact), glass transition.

**Thermochemical data**

The sublimation enthalpies of the species studied were calculated using the modified Trouton rule proposed recently [18]. In the case of ANDP (7) and 2-Nitro-1,3-dinitro-oxypropane **5** we used the melting points from our DSC experiments, for all other compounds – those estimated from the glass transition temperature values. In order to obtain the evaporation enthalpy for a particular liquid at room temperature, we used either the DSC melting enthalpy (in the case of ANDP) or the average value of the literature values -110 J/g for ANDP, SMX, PETN, ETN from this study and Ref 18 from the paper. Standard state enthalpies of formation listed in Table S1 were calculated as a combination of theoretical gas-phase values and empirically estimated sublimation/vaporization enthalpies. In the particular case of (6) the following isodesmic reaction was used:

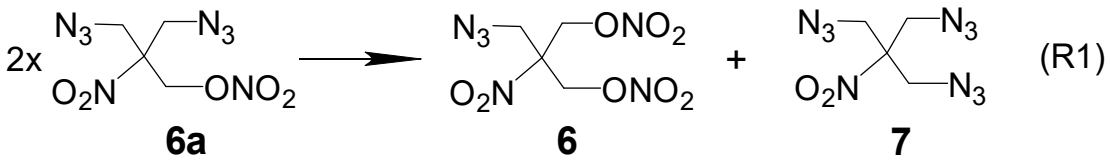


Combining the DLPNO-CCSD(T)/aVQZ enthalpy of this reaction 1.4 kJ/mol with the $\Delta_f H_m^0(gas)$ values of 510.3 and 922.0 kJ/mol obtained for (6a) and (7), respectively, using the atomization energies calculated using the W1-F12 multi-level procedure, finally we obtained the resulting $\Delta_f H_m^0(gas)$ of (6) to be 100 kJ/mol.

**Table S1.** The theoretically calculated gas-phase formation enthalpies $\Delta_f H_m^0(gas)$, empirically estimated sublimation/vaporization enthalpies $\Delta_{sub} H_m^0$ and resulting standard-state formation enthalpies $\Delta_f H_m^0$. All values are in kJ mol$^{-1}$.

| | Structure | | | | | |
|---|---|---|---|---|---|---|
| | ANDP (7) | SMX (2) | AMDNNM (6) | NIBTN (3) | NPN (4) | 2-Nitro-1,3-dinitro-oxypropane (5) |
| Formula | $C_4H_6N_{10}O_2$ | $C_6H_8N_6O_{16}$ | $C_4H_6N_6O_8$ | $C_4H_6N_4O_{11}$ | $C_3H_4N_4O_{10}$ | $C_3H_5N_3O_8$ |
| $\Delta_f H_m^0(gas)$ | 922 [a] | | 100 [b] | -308 [a] | -197 [a] | -227 [a] |
| $\Delta_{sub} H_m^0$ | 106 | | 95 | 94 | 83 | 121 |
| $\Delta_f H_m^0$ [c] | 816 | -542 [18] | 5 | -402 | -280 | -348 |

[a] Calculated using the W1-F12 multi-level procedure along with the atomization energy approach. [b] Calculated using the isodesmic reaction (R1). [c] Standard state enthalpy of formation calculated as a combination of theoretical gas-phase values and empirically estimated sublimation/vaporization enthalpies.

## NMR spectra

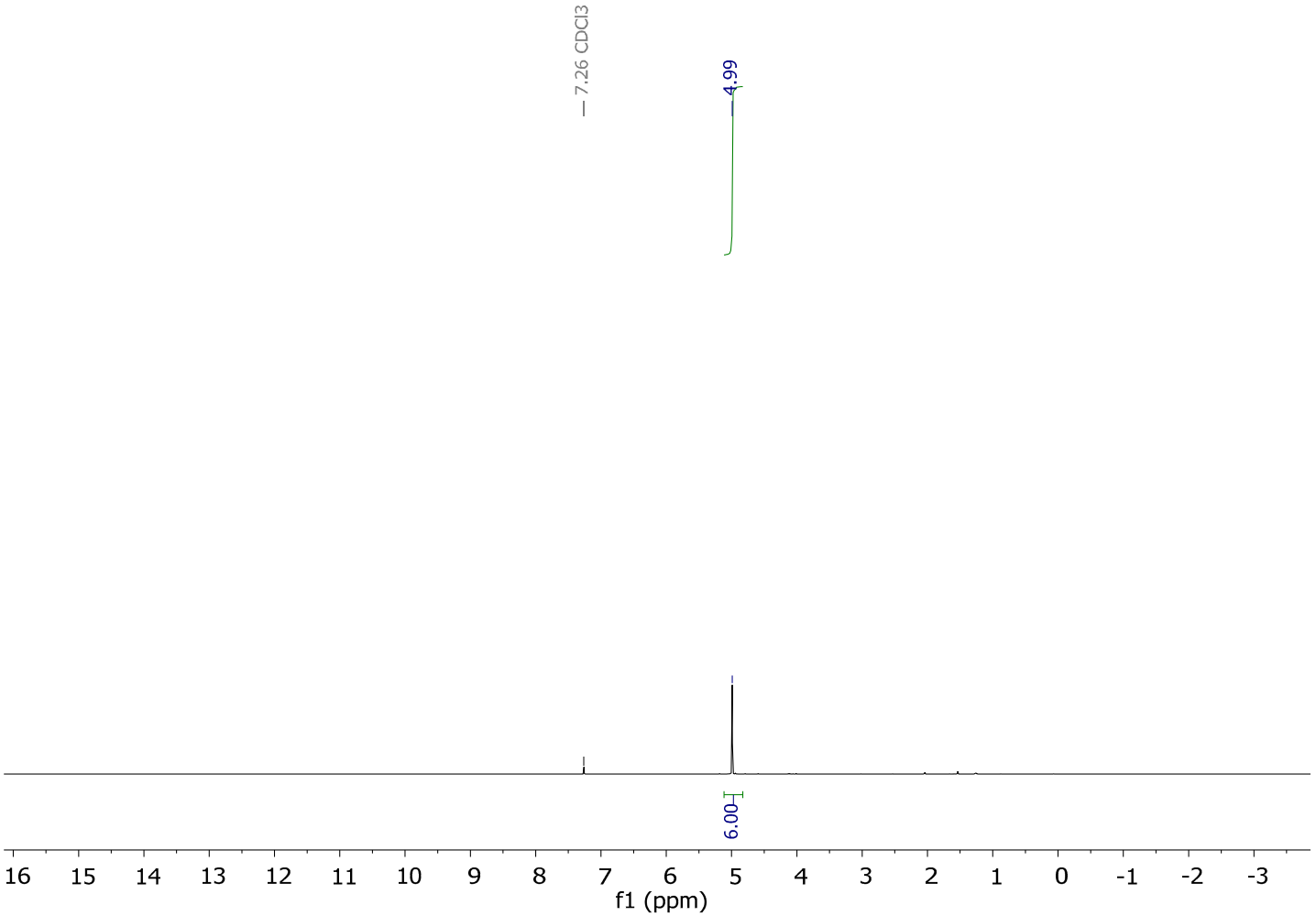


**Figure S5.** $^{1}H$ NMR (400 MHz, $CDCl_3$) spectra of trimethylol nitromethane trinitrate NIBTN (3).

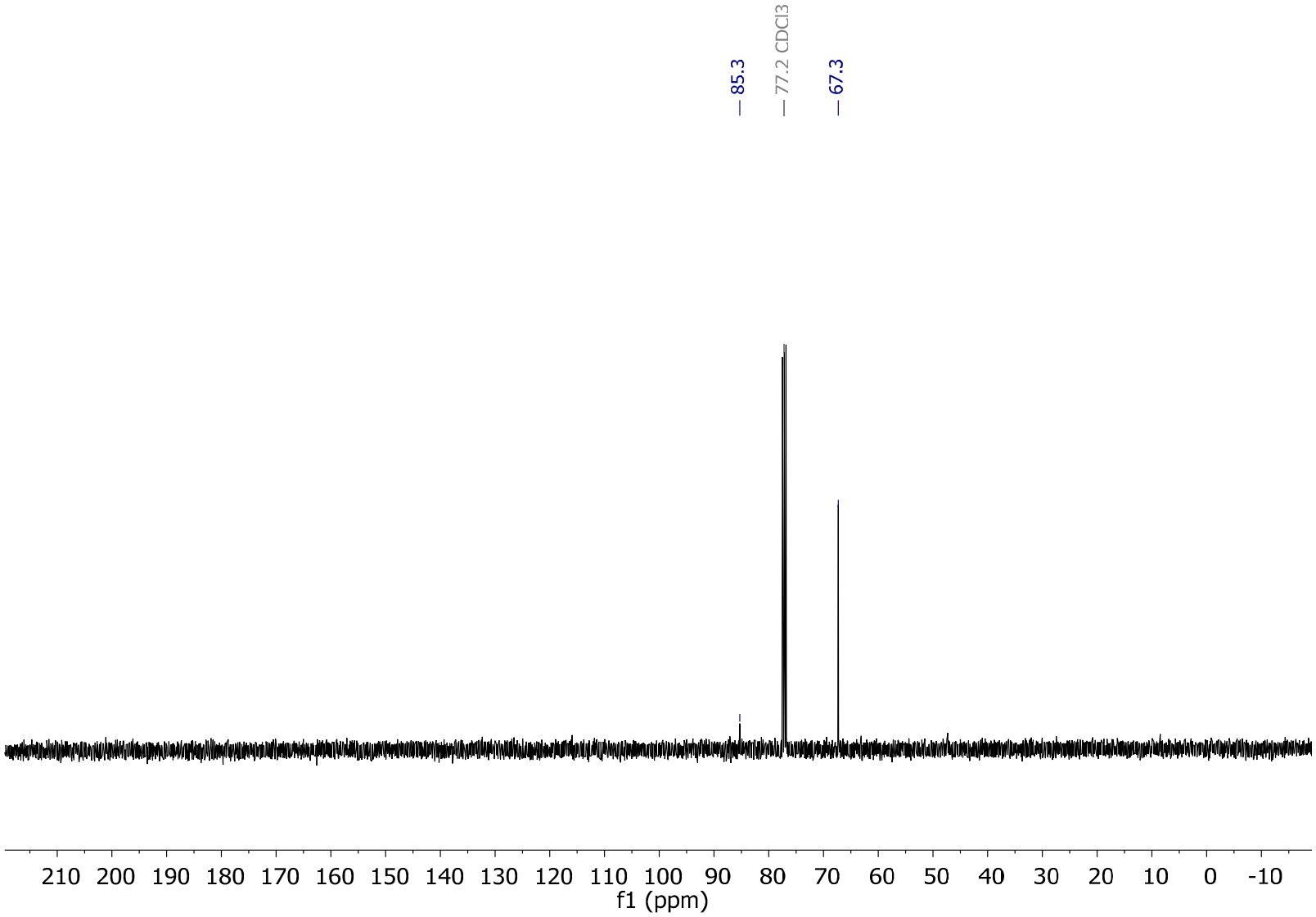


**Figure S6.** $^{13}C\{^{1}H\}$ NMR (101 MHz, $CDCl_3$) spectra of trimethylol nitromethane trinitrate NIBTN (3).

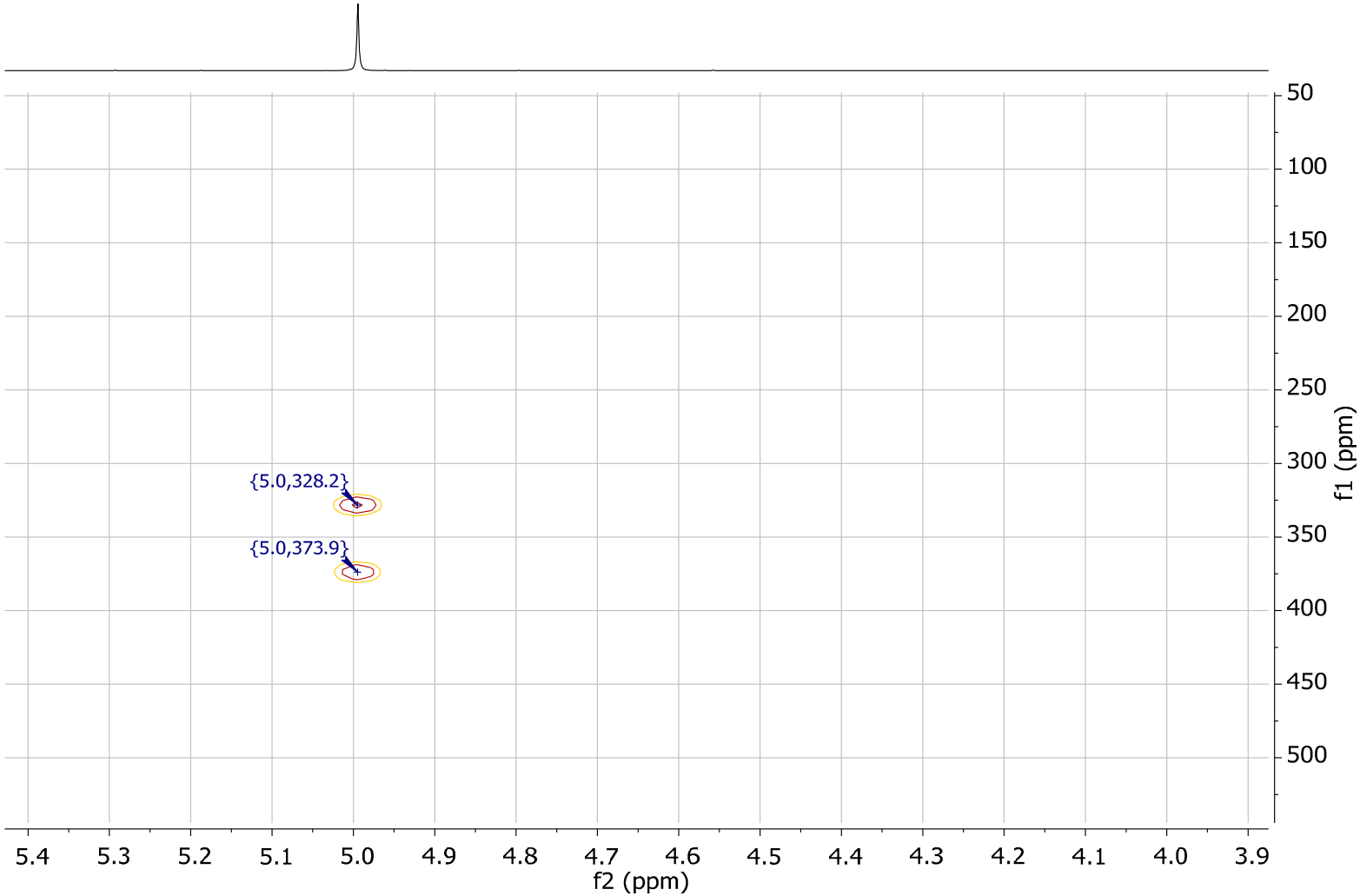


**Figure S7.** HMBC $^{1}H$-$^{15}N$ (400 MHz, 40.55 MHz, $CDCl_3$) spectra of NIBTN (3).

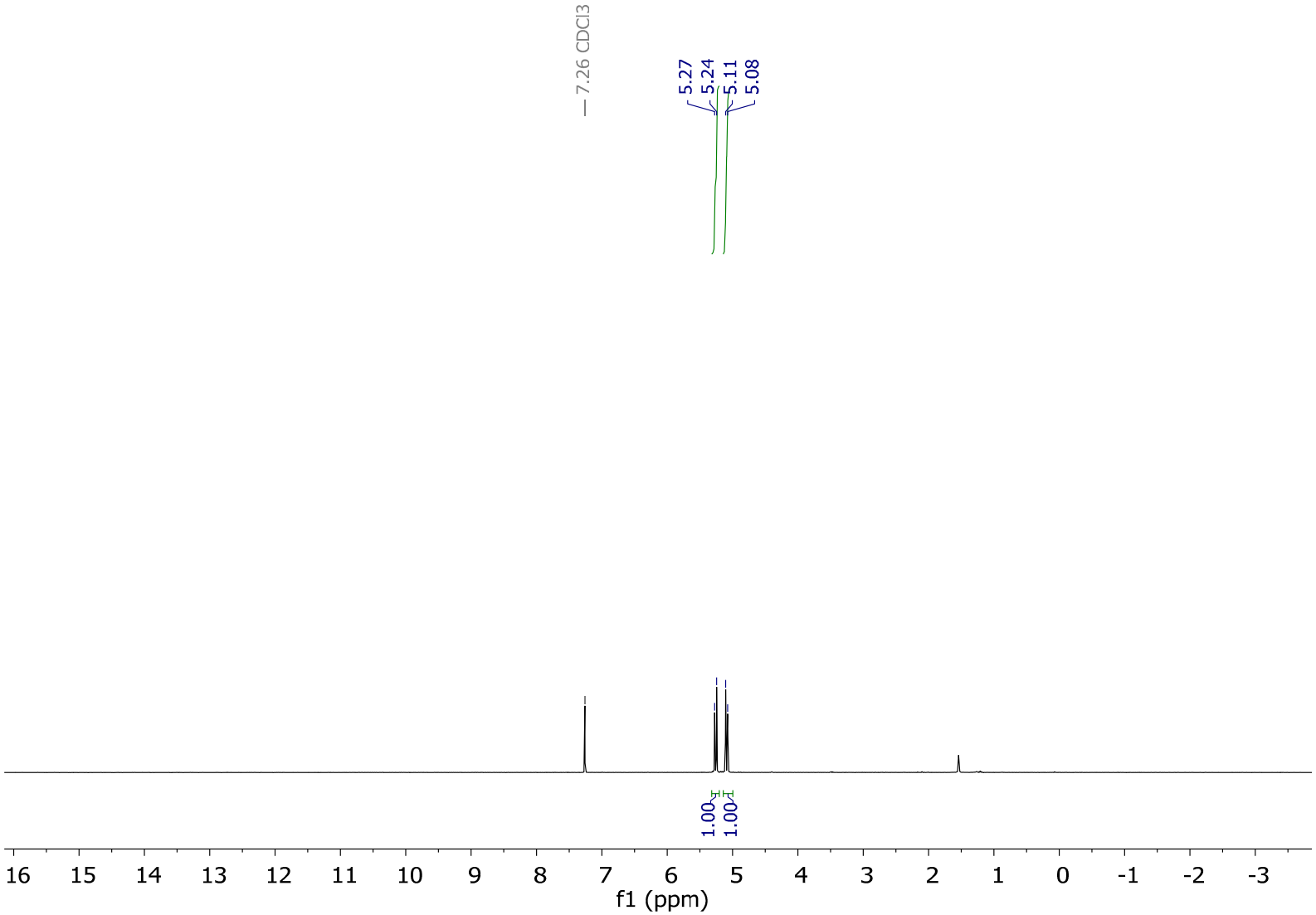


**Figure S8.** $^{1}H$ NMR (400 MHz, $CDCl_3$) spectra of SMX (2).

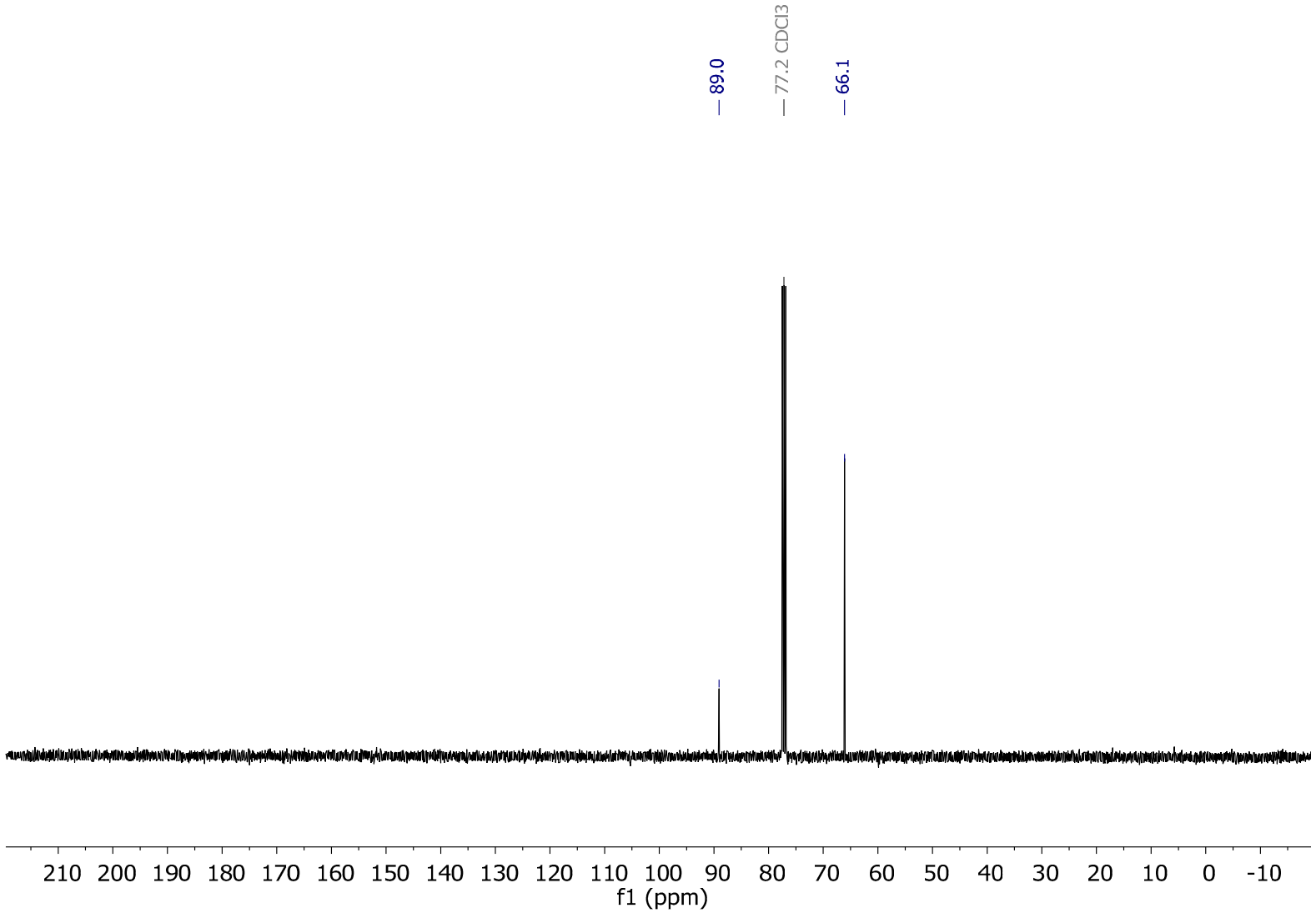


**Figure S9.** $^{13}C\{^{1}H\}$ NMR (101 MHz, $CDCl_3$) spectra of SMX (2).

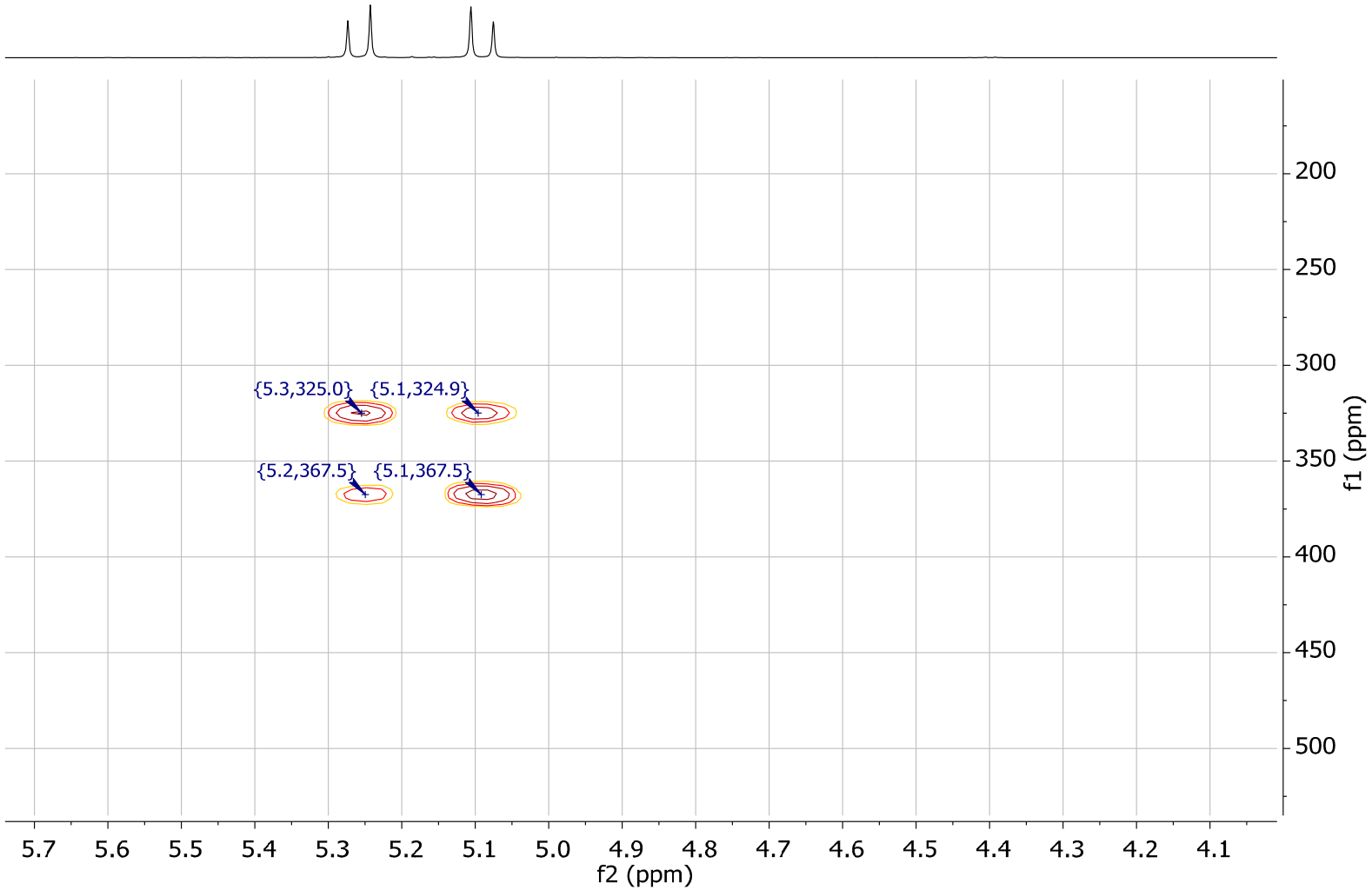


**Figure S10.** HMBC $^{1}H$-$^{15}N$ (400 MHz, 40.55 MHz, $CDCl_3$) spectra of SMX (2).

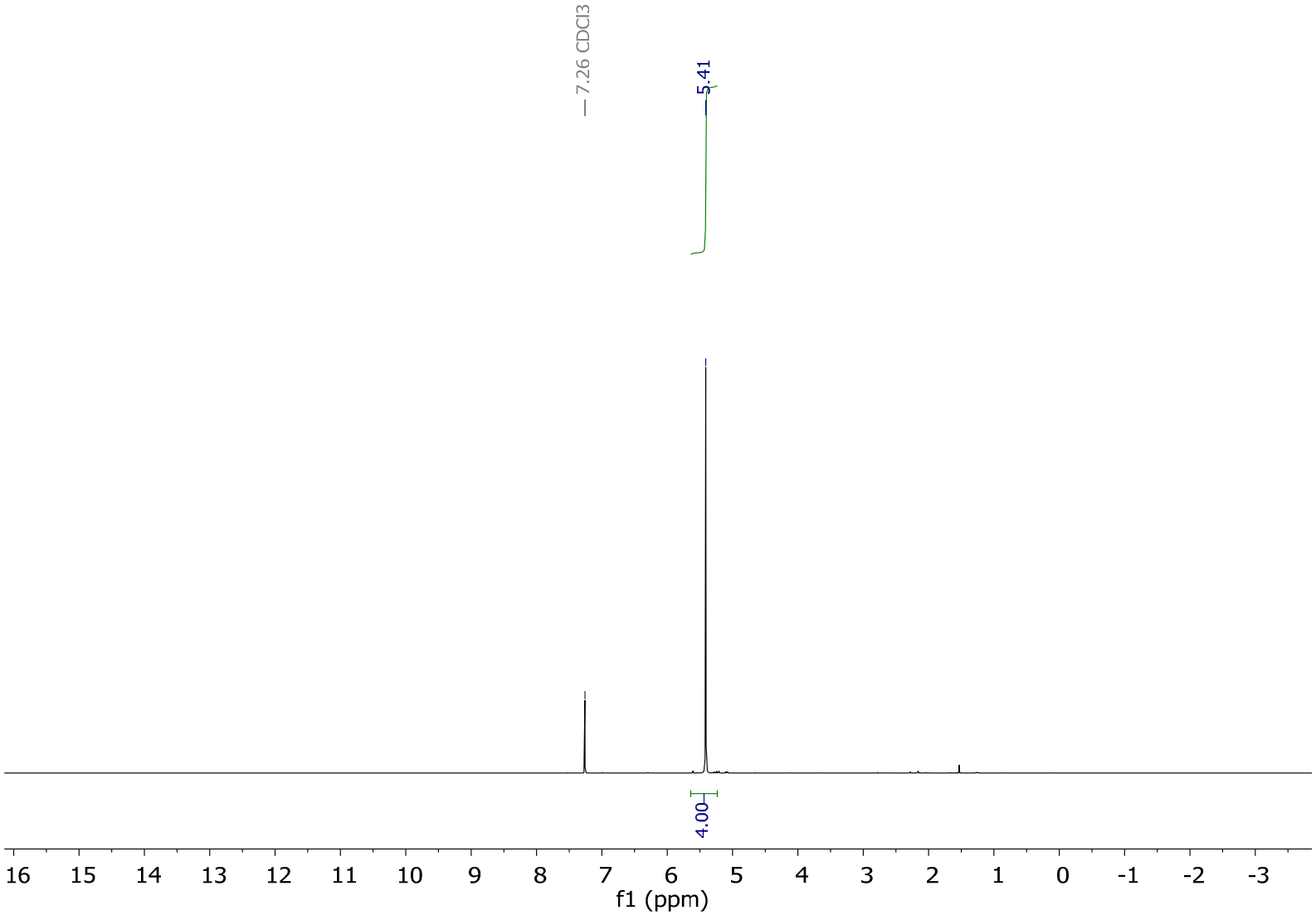


**Figure S11.** $^{1}$H NMR (400 MHz, $CDCl_3$) spectra of 2,2-dinitropropane-1,3-diyl dinitrate (NPN) **4.**

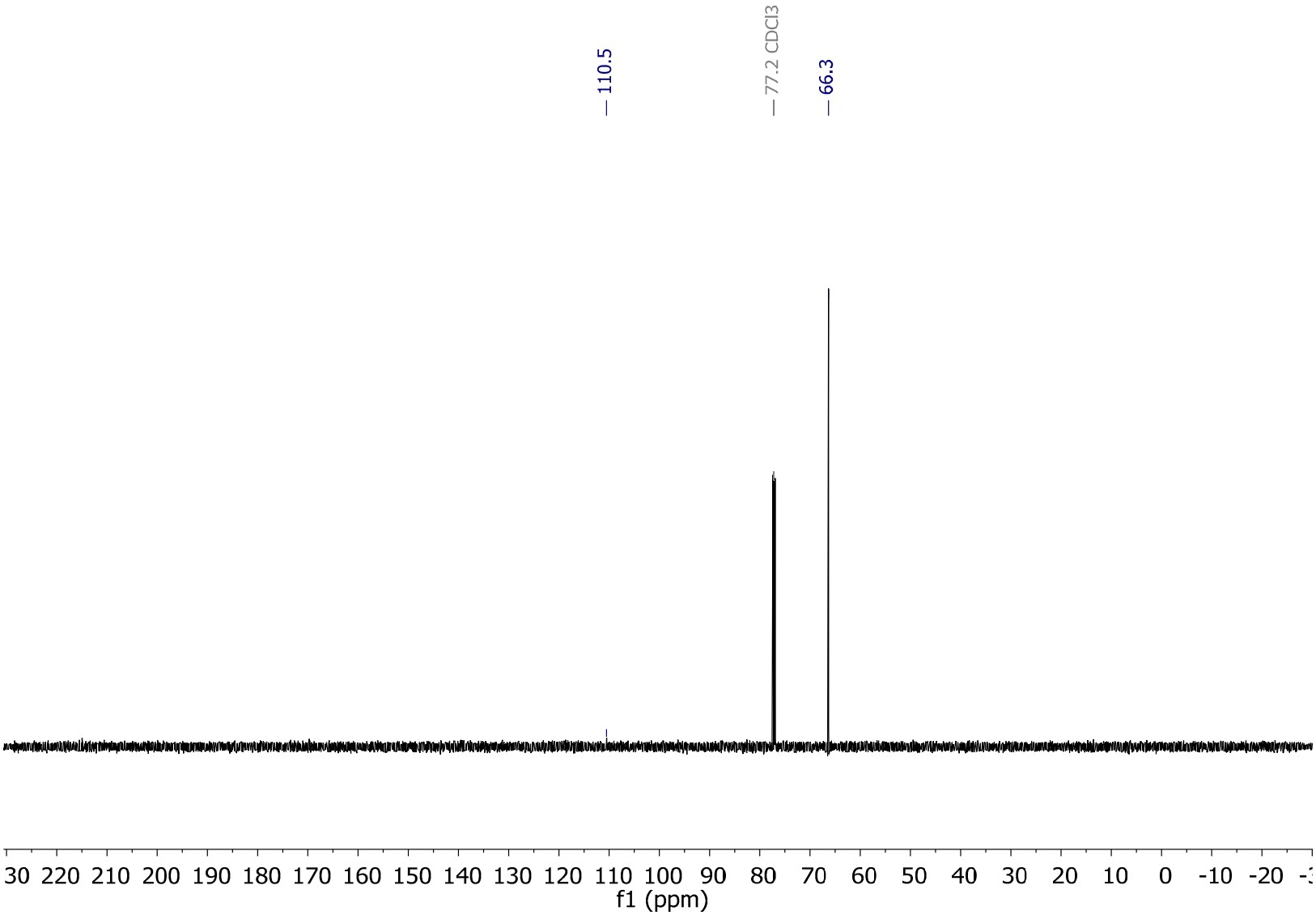


**Figure S12.** $^{13}C\{^{1}H\}$ NMR (101 MHz, $CDCl_3$) spectra of 2,2-dinitropropane-1,3-diyl dinitrate (NPN) **4.**

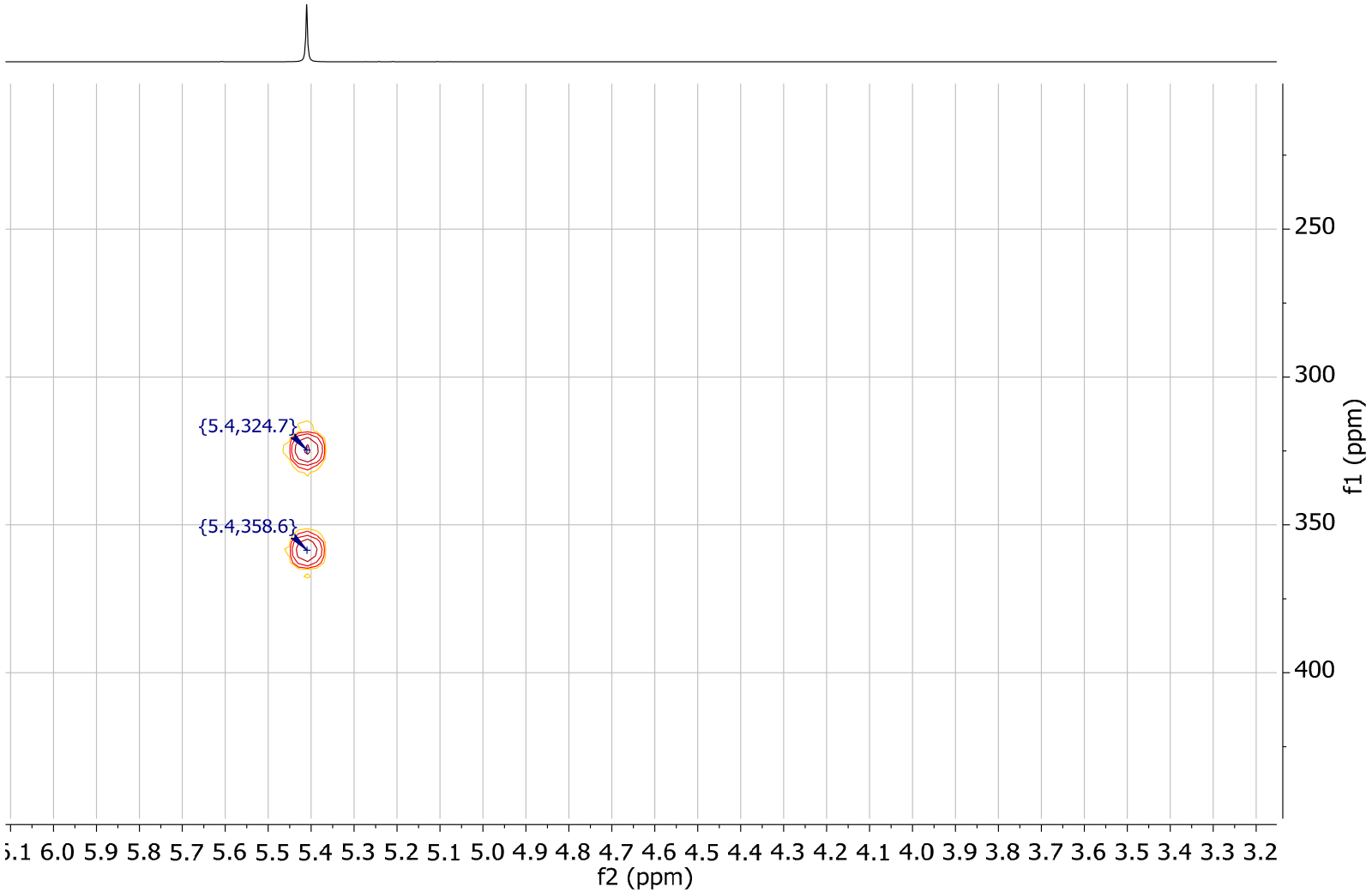


**Figure S13.** HMBC $^{1}H$-$^{15}N$ (400 MHz, 40.55 MHz, $CDCl_3$) spectra of 2,2-dinitropropane-1,3-diyl dinitrate (NPN) **4.**

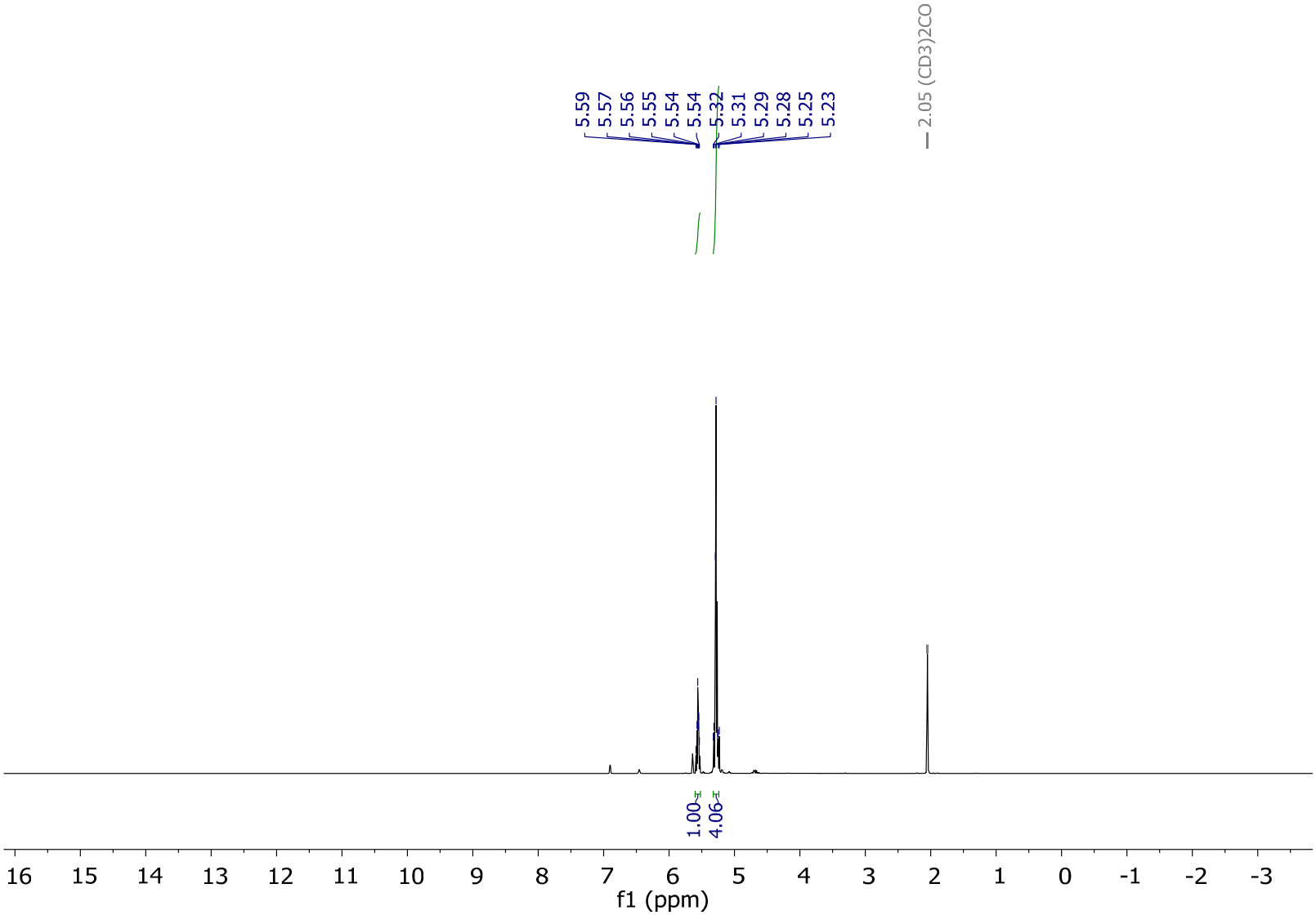


**Figure S14.** [1]H NMR (400 MHz, acetone-d6) spectra of 2-nitro-1,3-dinitrooxypropane (5).

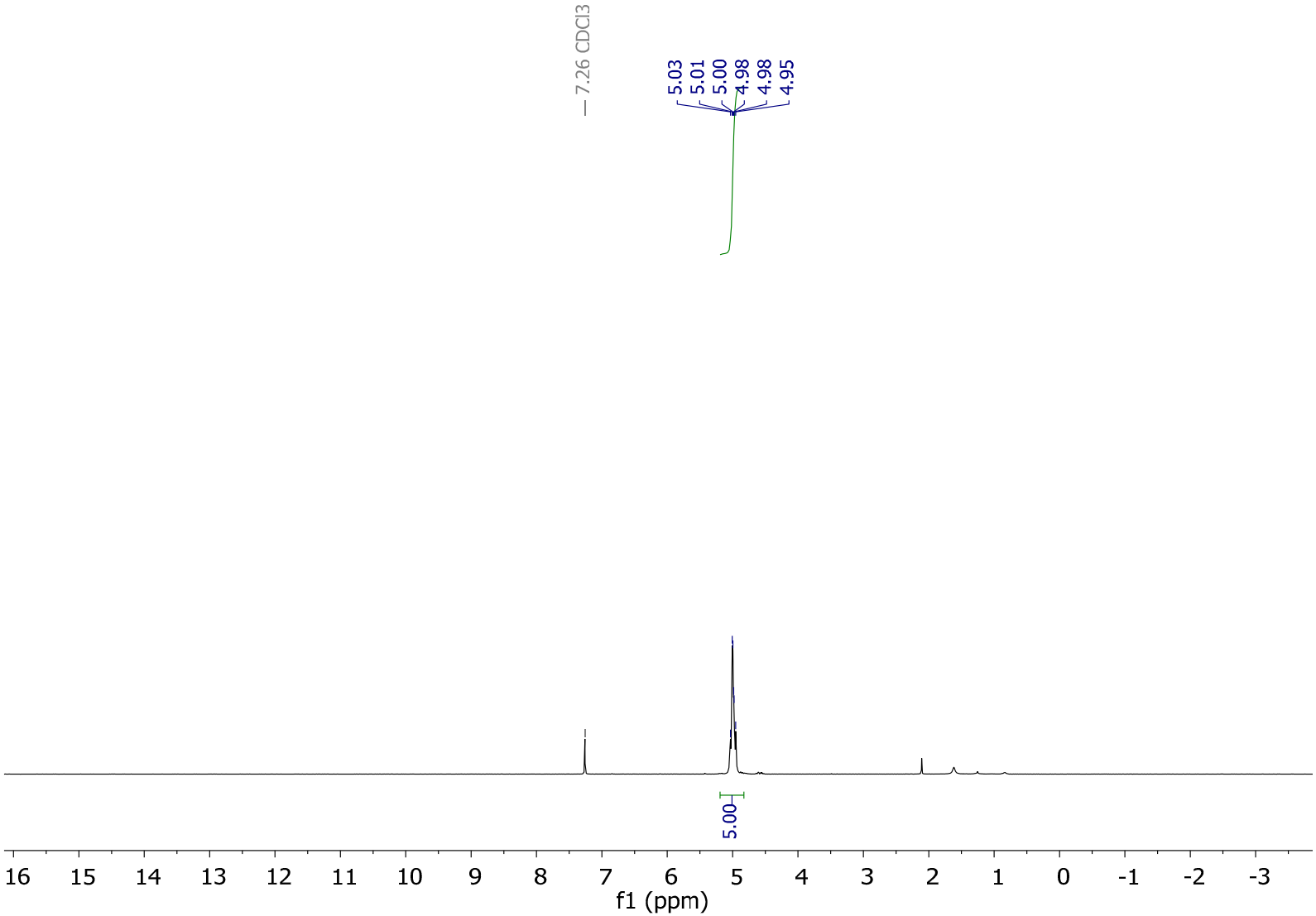


**Figure S15.** $^{1}H$ NMR (400 MHz, $CDCl_3$) spectra of 2-nitro-1,3-dinitrooxypropane **5.**

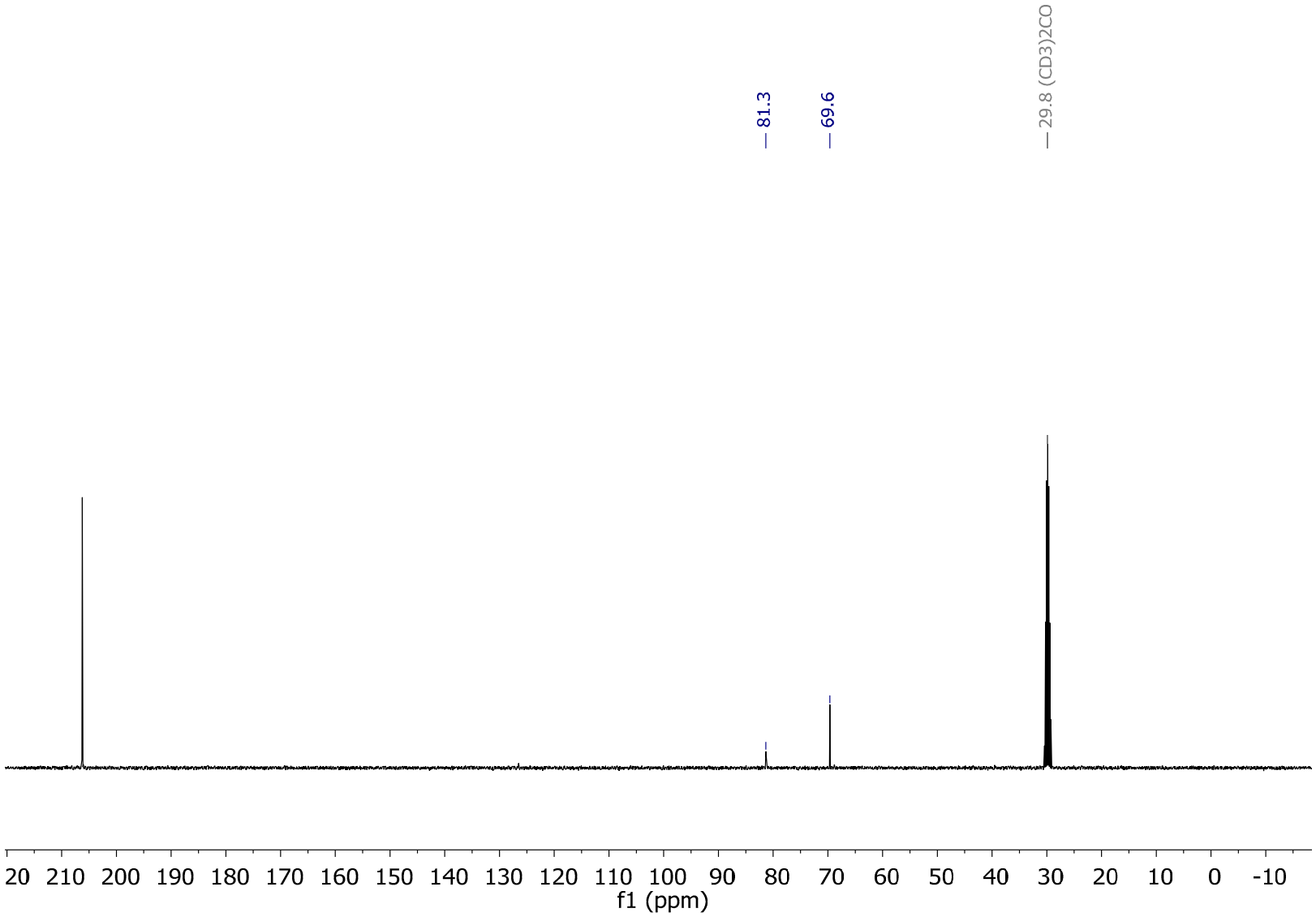


**Figure S16.** $^{13}C\{^{1}H\}$ NMR (101 MHz, acetone-d6) spectra of 2-nitro-1,3-dinitrooxypropane (5).

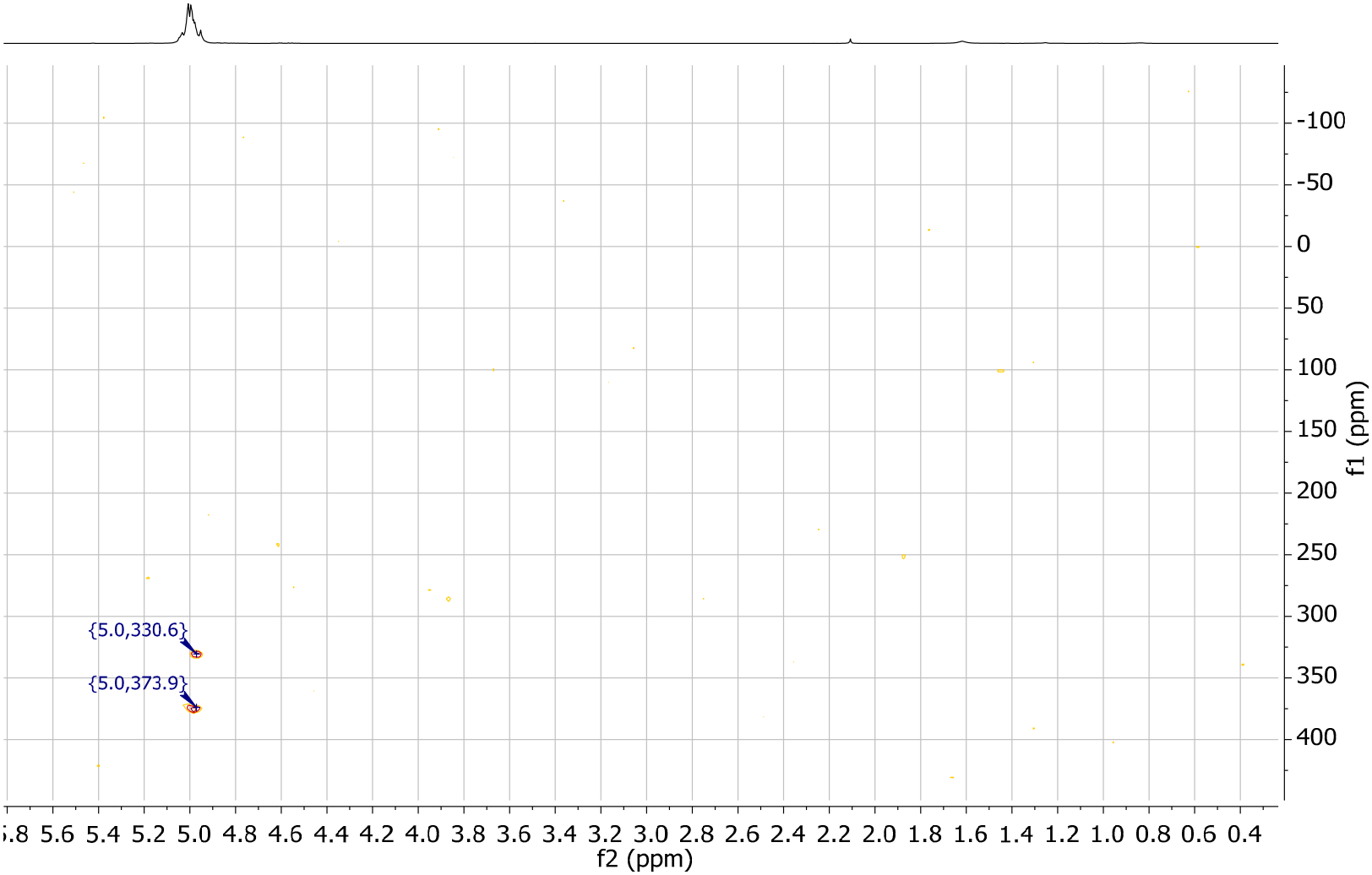


**Figure S17.** HMBC $^{1}H$-$^{15}N$ (400 MHz, 40.55 MHz, $CDCl_3$) spectra of 2-nitro-1,3-dinitrooxypropane (5).

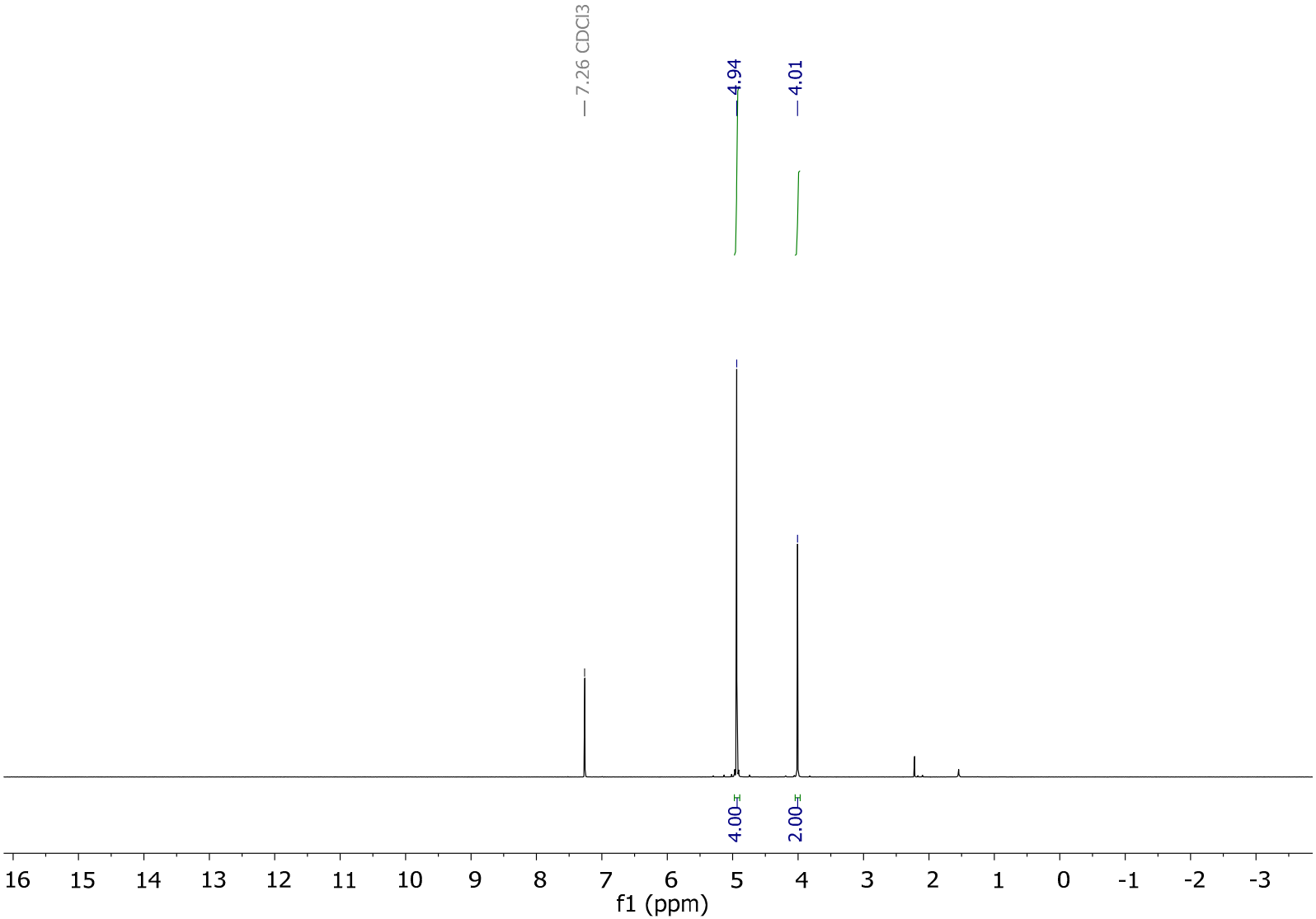


**Figure S18.** $^{1}H$ NMR (400 MHz, $CDCl_3$) spectra of AMDNNM (6).

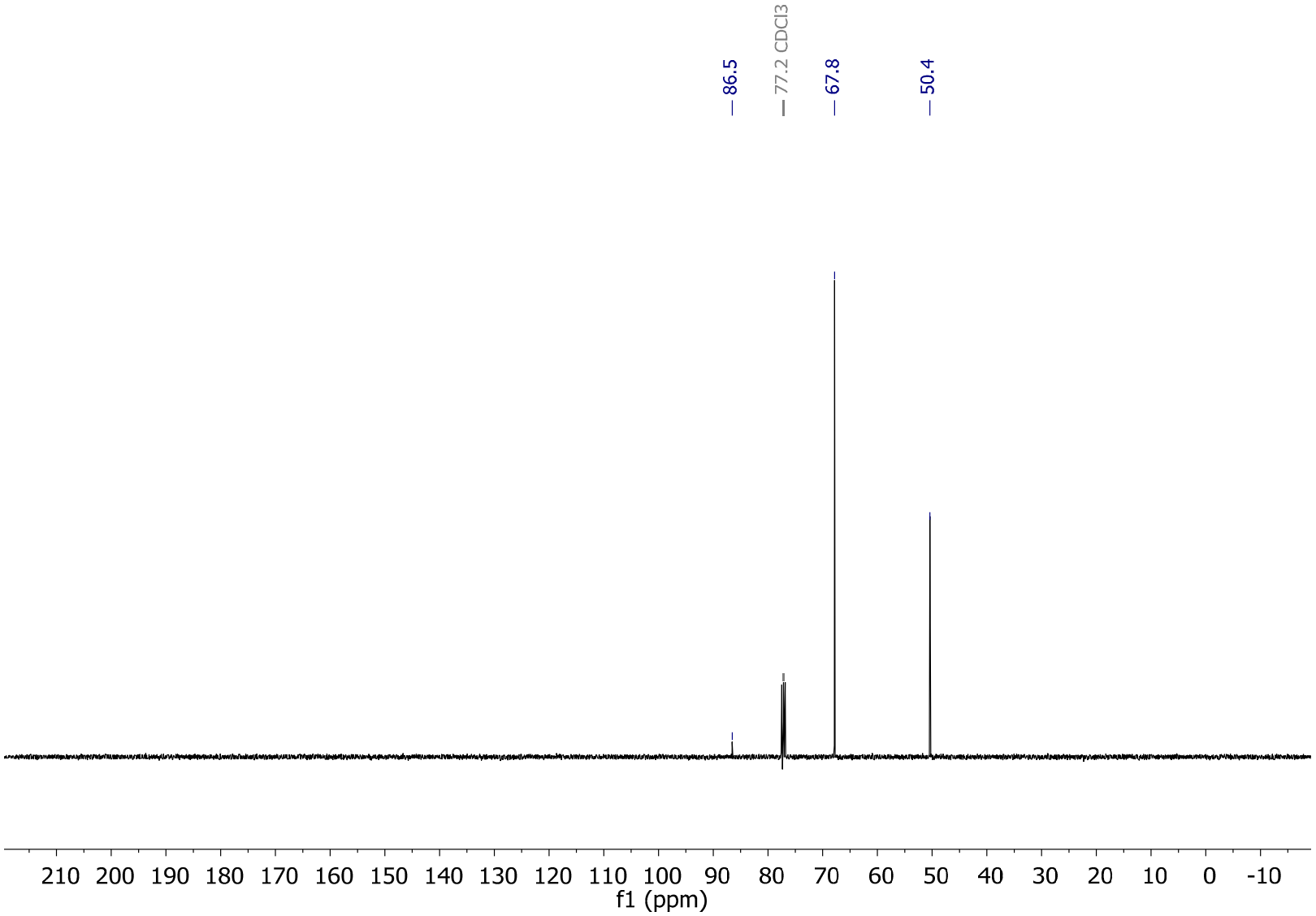


**Figure S19.** $^{13}C\{^{1}H\}$ NMR (101 MHz, $CDCl_3$) spectra of AMDNNM (6).

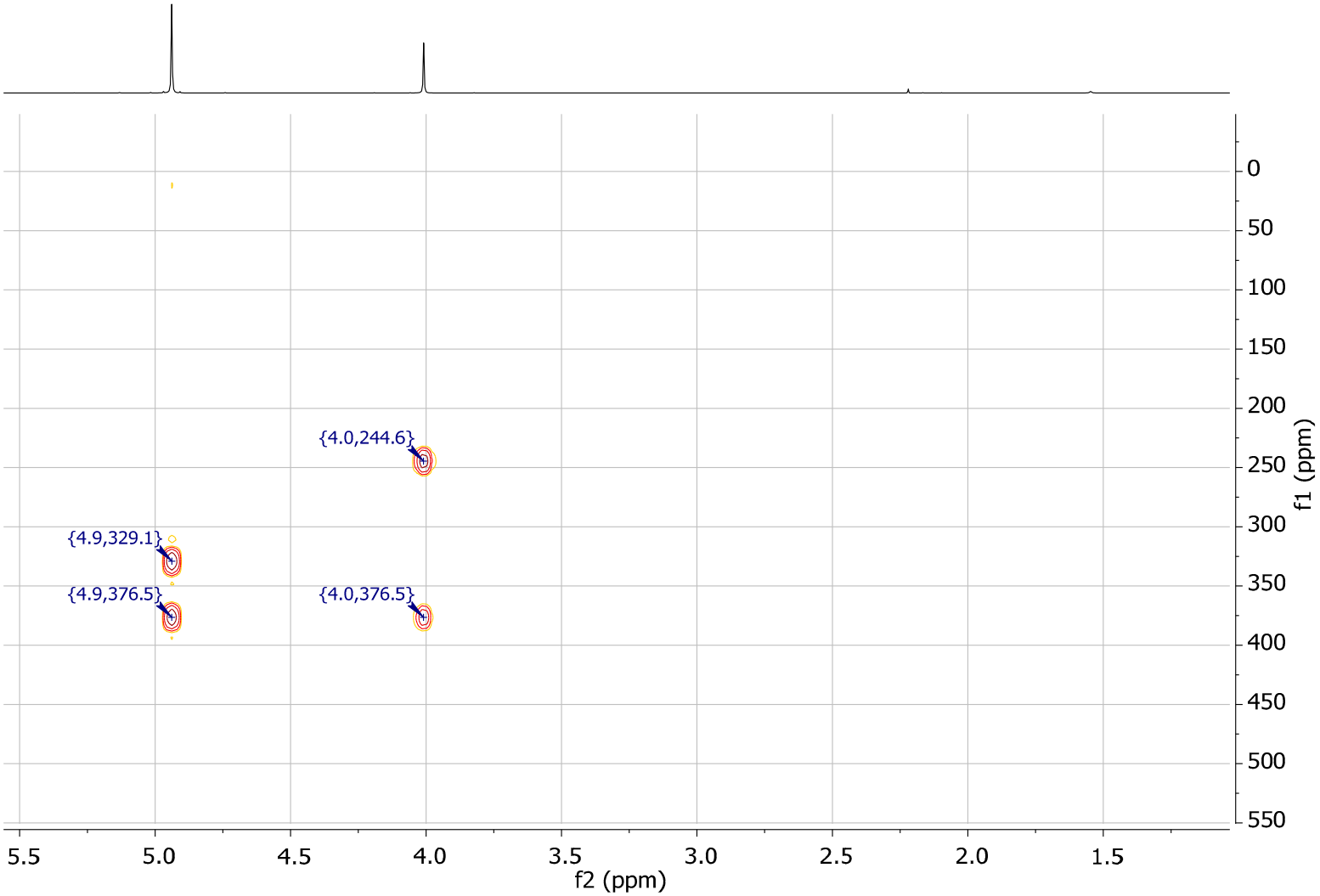


**Figure S20.** HMBC $^{1}H$-$^{15}N$ (400 MHz, 40.55 MHz, $CDCl_3$) spectra of AMDNNM (6).

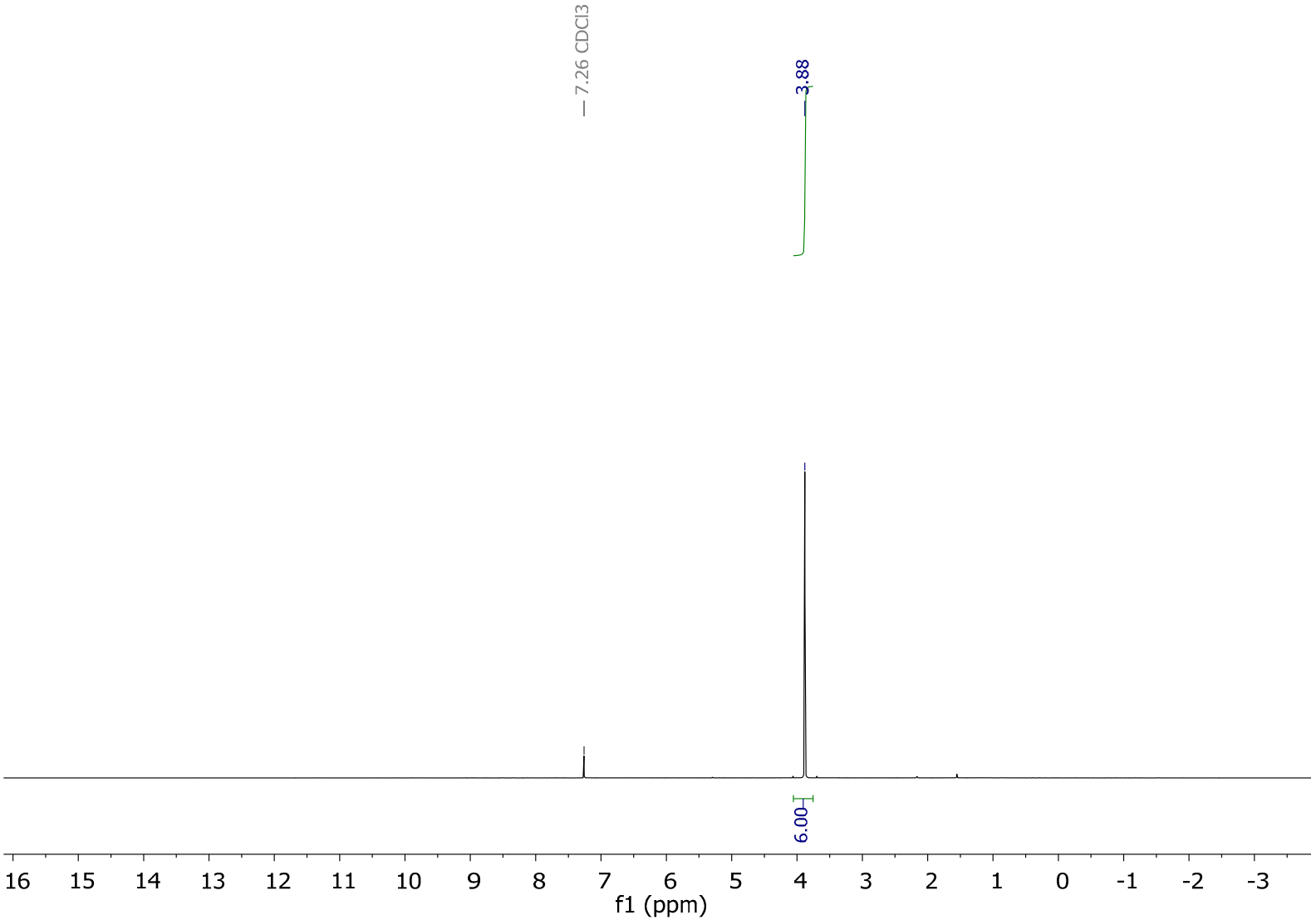


**Figure S21.** $^{1}$H NMR (400 MHz, $CDCl_3$) spectra of 1,3-diazido-2-(azidomethyl)-2-nitropropane (ANDP) **7.**

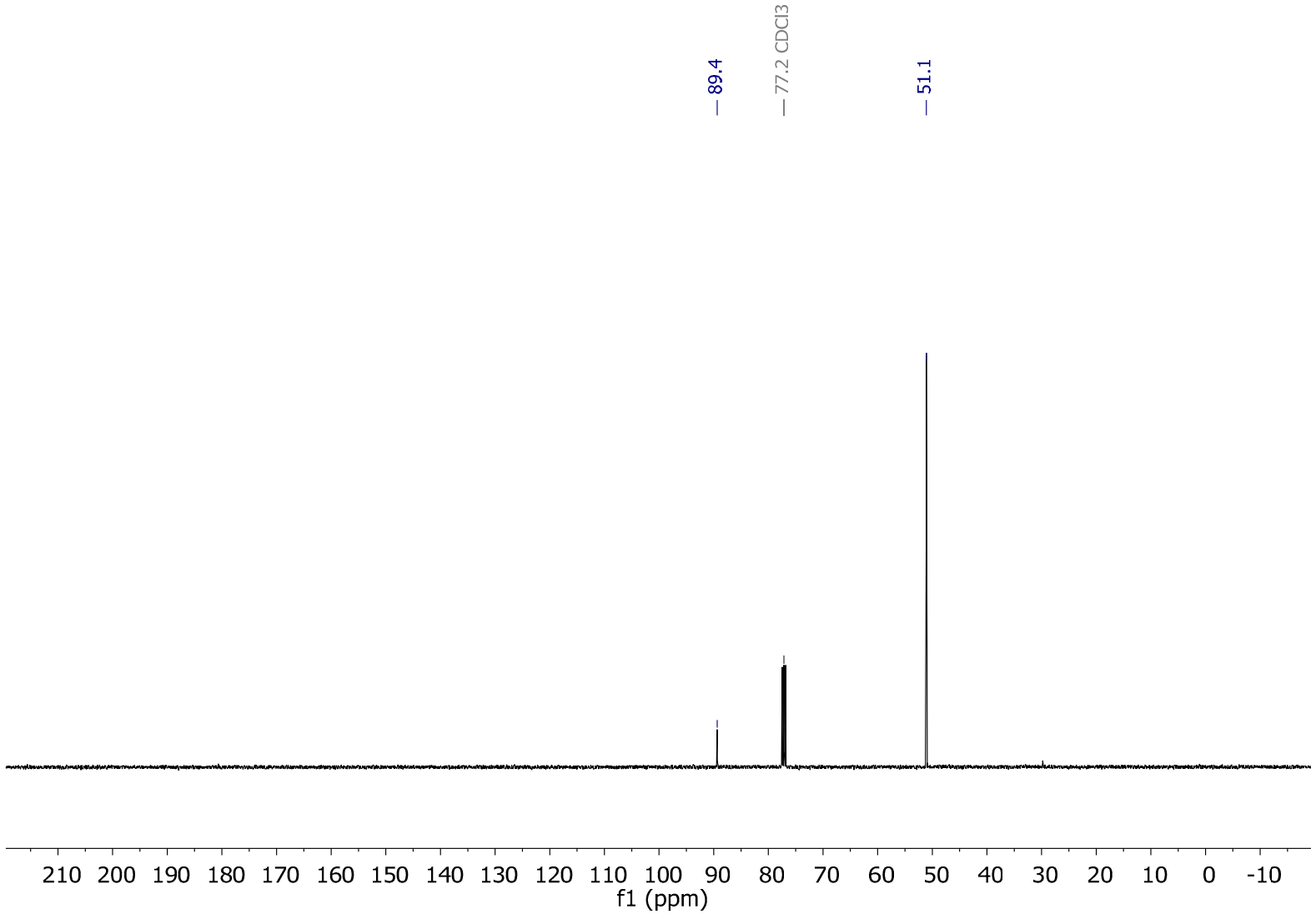


**Figure S22.** $^{13}C\{^{1}H\}$ NMR (101 MHz, $CDCl_3$) spectra of 1,3-diazido-2-(azidomethyl)-2-nitropropane (ANDP) **7.**

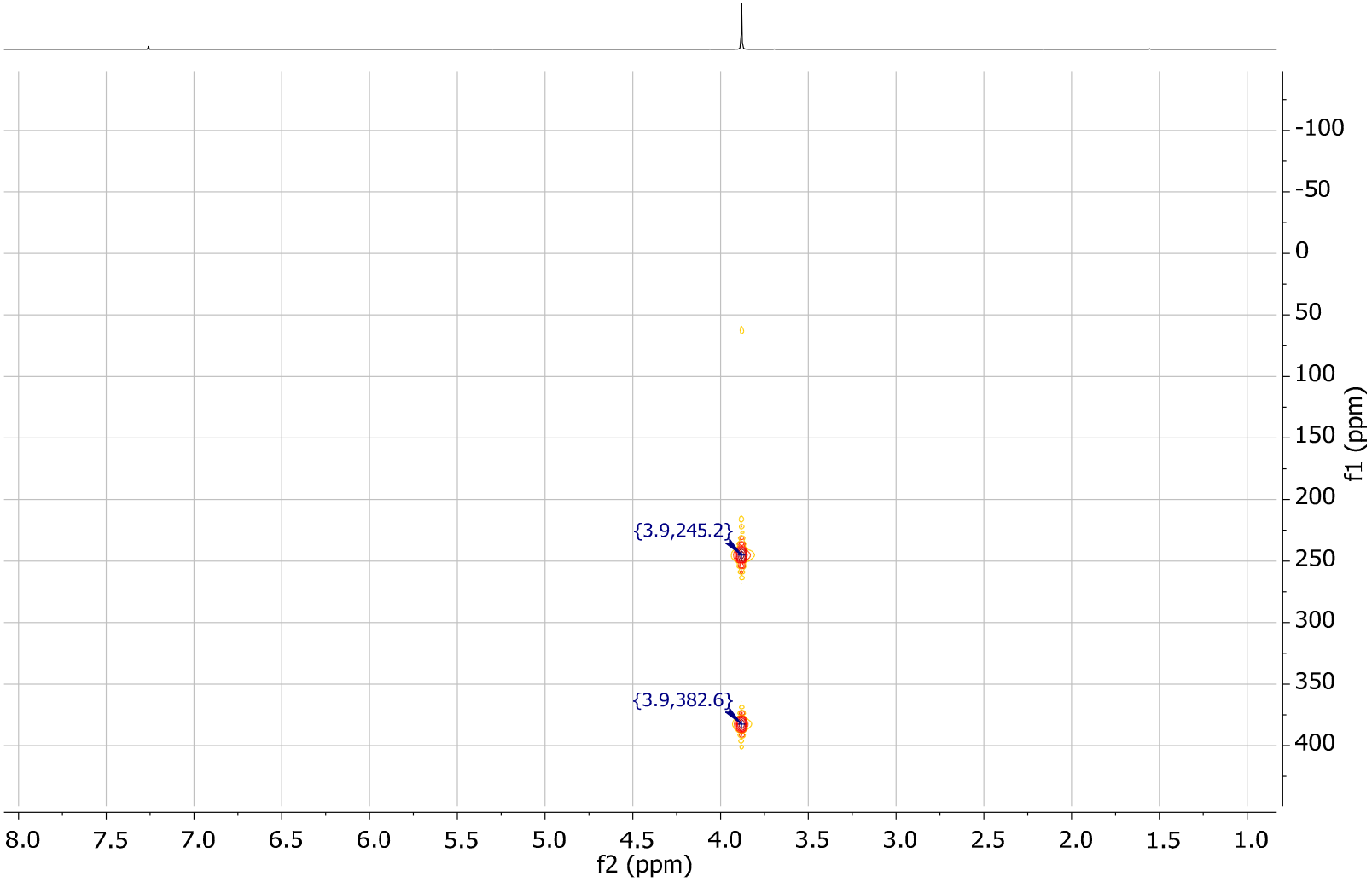


**Figure S23.** HMBC $^{1}H$-$^{15}N$ (400 MHz, 40.55 MHz, $CDCl_3$) spectra of 1,3-diazido-2-(azidomethyl)-2-nitropropane (ANDP) **7**.